

Effect of yttrium on improvement of dielectric properties and magnetic switching behavior in
 BiFeO_3

This article has been downloaded from IOPscience. Please scroll down to see the full text article.

2008 J. Phys.: Condens. Matter 20 045218

(<http://iopscience.iop.org/0953-8984/20/4/045218>)

View [the table of contents for this issue](#), or go to the [journal homepage](#) for more

Download details:

IP Address: 129.252.86.83

The article was downloaded on 29/05/2010 at 08:04

Please note that [terms and conditions apply](#).

Effect of yttrium on improvement of dielectric properties and magnetic switching behavior in BiFeO₃

R K Mishra¹, Dillip K Pradhan¹, R N P Choudhary^{1,3} and A Banerjee²

¹ Department of Physics and Meteorology, IIT Kharagpur-721302, India

² UGC-DAE Consortium for Scientific Research, University Campus, Khandwa Road, Indore-452017, India

E-mail: crnpfl@phy.iitkgp.ernet.in

Received 19 October 2007, in final form 4 December 2007

Published 8 January 2008

Online at stacks.iop.org/JPhysCM/20/045218

Abstract

Yttrium (Y) modified nanocrystalline samples of BiFeO₃ (BFO) were prepared by a metal ion ligand complex-based precursor-solution evaporation method. Partial substitution of Y (0–15%) at the Bi site results in structural change (rhombohedral to tetragonal) and single phase formation. With increasing Y concentration, enhancement in dielectric ordering, reduction in loss tangent and improvement in magnetic ordering in BFO were observed. Diffuse peaks in both permittivity and loss tangent were observed at 207 °C and 222 °C, respectively, for 15% substitution of Y. In all the Y substituted BFO samples, a switching behavior in low fields was observed in the field dependence of magnetization, even at room temperature, and this behavior was found to be improved with increasing Y concentration.

(Some figures in this article are in colour only in the electronic version)

1. Introduction

Although known for a long time, the enigma of multiferroics is yet to be solved by scientists due to the intriguing physics it involves. The existence of simultaneous electric and magnetic ordering (in the same phase) has made these materials useful for future technology in the field of information storage and sensors [1, 2]. Looking at the many past discoveries in this field one will find that BiFeO₃ (BFO) with a distorted perovskite (ABO₃) structure is a fascinating multiferroic material because of its ferroelectric transition and antiferromagnetic Néel temperature well above the room temperature [3]. However, BFO has some inherent problems such as preparation of the phase pure compound, a high leakage current, lower magnetoelectric coupling coefficients and wide difference in ferroic transition temperatures (T_c/T_N) [4–7]. Recently different synthesis processes have been adopted to get single phase formation of BFO, and with this improved synthesis process very high values of polarization can be achieved [8, 9]. However, in pure BFO ceramics high value macroscopic

magnetization could not be achieved. Several attempts have been made to solve these problems by suitable modifications at the Bi and/or Fe sites or fabrication of composites [10–17]. It is found that some rare earth ions substituted at the Bi site have reduced leakage current and Curie temperature and improved dielectric ordering and structural stability etc [11–17].

The weak magnetic characteristics of BFO are attributed to some factors such as spiral spin structure, orientation of magnetic moments perpendicular to the rhombohedral axis and magnetic moment canting [18]. Bi substitution by rare earth ions improves magnetic properties attributed to structural phase transition, resulting in the release of latent magnetization [19–21].

It seems logical to attribute, in general, the changes in multiferroic properties on Bi substitution by a rare earth to the cation size effect. If so, the hypothesis should be valid for substitution of Bi (ionic radius = 1.03 Å) by a non-rare earth ion Y having an ionic radius (ionic radius = 0.90 Å) comparable to that of reported rare earth substituents. Uchinda *et al* [14] have made a comparative study of the substitutional effect of two rare earths (i.e. La and Nd) at the Bi site of BFO and found that both have produced compositional driven

³ Author to whom any correspondence should be addressed.

structural change affecting the ferroelectric properties. Also, it has been established that both La and Nd substitution suppress the inhomogeneous spin structure in BFO thereby enhancing its magnetic property. It is worth mentioning here that the La^{3+} ion has an electronic configuration unlike that of Nd^{3+} , which has unpaired electron in its f-orbital, but both can enhance the multiferroic properties of BFO. The Y^{3+} ion, which has an electronic configuration closer to that of La^{3+} (both belong to the d-block) but an ionic radius comparable to ions of f-block elements like Nd^{3+} , Dy^{3+} etc, seems to be an interesting candidate for substitution at the Bi site of BFO. Moreover, owing to the intrinsic ferromagnetic properties of YFeO_3 [22, 23], it seems quite plausible to try the solid solution of YFeO_3 with BiFeO_3 for any possible enhancement of multiferroic properties. Also a gradual reduction of the Goldsmith tolerance factor (t) is found from calculation with Y substitution in BFO, i.e. $\text{Bi}_{1-x}\text{Y}_x\text{FeO}_3$ (BYFO) and the values of t are 0.9146, 0.9133, 0.9120 and 0.9107 for $x = 0, 0.05, 0.10$ and 0.15 , respectively. With this aim in mind, we have made a systematic study on the effect of Y on the structural, dielectric and magnetic properties of BFO over a small concentration (0–15%).

2. Experimental details

The nanosized powders of $\text{Bi}_{1-x}\text{Y}_x\text{FeO}_3$ (BYFO) ($x = 0, 0.05, 0.1, 0.15$) were prepared by a metal ion ligand complex-based precursor-solution evaporation method using $\text{Bi}(\text{NO}_3)_3 \cdot 5\text{H}_2\text{O}$, $\text{Fe}(\text{NO}_3)_3 \cdot 9\text{H}_2\text{O}$ and a solution of Y_2O_3 in HNO_3 . Triethylene amine (TEA) was added as a complexing agent. A homogeneous solution of precursors in the appropriate molar ratio was processed to obtain sample powders, and the latter were calcined at optimized temperatures of 600, 700 and 750 °C for $x = 0, 0.05, 0.10, 0.15$, respectively, for 6 h. The cold-pressed pellets were sintered at (optimized temperatures) 50 °C higher than their respective calcination temperatures. The preliminary structural analysis was carried out using x-ray diffraction (XRD) data collected in a wide range of Bragg angles 2θ ($20^\circ \leq 2\theta \leq 80^\circ$) at room temperature with an x-ray powder diffractometer (Rigaku, Miniflex, Japan). The nanocrystalline nature of the samples was studied with a transmission electron microscope (TEM) (JEOL, JEM 2100). Fourier transform infrared (FTIR) spectra of all the samples were recorded with a FTIR spectrometer (Thermo Nicolet Corporation, NEXUS-870) in the mid frequency range with a resolution of 2 cm^{-1} . Electrical measurements were carried out on a cell, Ag|pellet|Ag, in the frequency range of 100 Hz–1 MHz using a LCR Hi Tester (model HIOKI 3532) up to 350 °C. The P – E hysteresis loops were obtained on the poled samples using a precision workstation (m/s Radiant Technologies, Inc.). Magnetic measurements were carried out using a 14 T Quantum Design PPMS-VSM in the temperature range from 2 to 300 K.

3. Results and discussion

Figure 1 shows the room temperature XRD pattern of $\text{Bi}_{1-x}\text{Y}_x\text{FeO}_3$ ($x = 0, 0.05, 0.1, 0.15$). All the peaks of

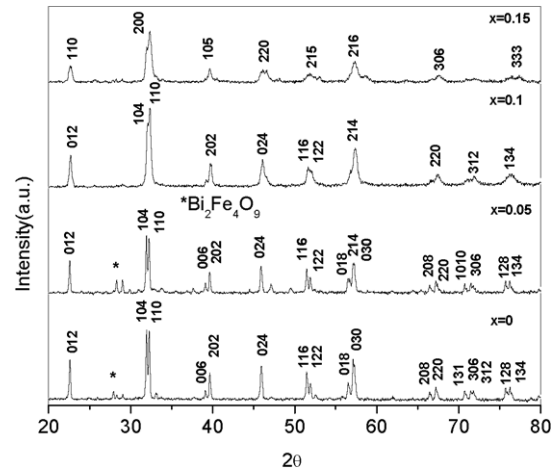


Figure 1. Room temperature XRD pattern of $\text{Bi}_{1-x}\text{Y}_x\text{FeO}_3$.

the patterns were indexed in different crystal systems and cell configurations with observed peak position, i.e. Bragg angle (2θ) and interplanar spacing (d), using a computer software POWDMULT [24]. On the basis of best agreement between observed and calculated values of d and 2θ it is found that for $x \leq 0.1$ the structure is rhombohedral, and for $x = 0.15$ the structure changes to tetragonal. The least square refined lattice parameters (equivalent hexagonal for $x \leq 0.10$) of $\text{Bi}_{1-x}\text{Y}_x\text{FeO}_3$ are: for $x = 0$, $a = 5.5655 \text{ \AA}$, $c = 13.8280 \text{ \AA}$, for $x = 0.05$, $a = 5.5548 \text{ \AA}$, $c = 13.8452 \text{ \AA}$, for $x = 0.1$, $a = 5.5521 \text{ \AA}$, $c = 13.7343 \text{ \AA}$ and for $x = 0.15$, $a = 5.5619 \text{ \AA}$, $c = 12.5305 \text{ \AA}$. The lattice strain and crystallite size were calculated by the variance method [25]. Assuming that the broadening of the x-ray diffraction line profile is due to the crystallite size and lattice strain, the variance of the profile [26] can be expressed as

$$W(2\theta) = \frac{\lambda \times \Delta(2\theta)}{2\pi^2 p' \cos \theta} + 4 \tan^2 \theta \langle e^2 \rangle$$

where $\Delta(2\theta)$ is the angular range, p' is the crystallite size, λ is the x-ray wavelength, $\langle e^2 \rangle$ is the mean square strain and 2θ is the Bragg angle.

Using this formula we calculated the lattice strain of the $\text{Bi}_{1-x}\text{Y}_x\text{FeO}_3$ compounds as 0.00131, 0.00179, 0.00238 (along [012]) for $x = 0, 0.05, 0.10$, respectively, and 0.00237 (along [110]) for $x = 0.15$. The crystallite sizes were found to be 43 nm, 48 nm, 19 nm and 17 nm for $x = 0, 0.05, 0.10$ and 0.15 , respectively. The crystallite size gradually decreases with increasing concentration of Y whereas the lattice strain gradually increases up to $x = 0.10$ and slightly decreases for $x = 0.15$.

As evident from the figure there is a systematic change in number of peaks with increasing percentage of Y substitution. A small amount of secondary phase was observed in BFO ($x = 0$). This secondary phase was due to $\text{Bi}_2\text{Fe}_4\text{O}_9$. It became more prominent for $x = 0.05$ and finally vanished for $x \geq 0.10$ leading to single phase formation at higher concentrations of Y in BYFO. Also it is evident from figure 1 that the doubly split peaks like (104), (110) and (006), (202) merge partially to

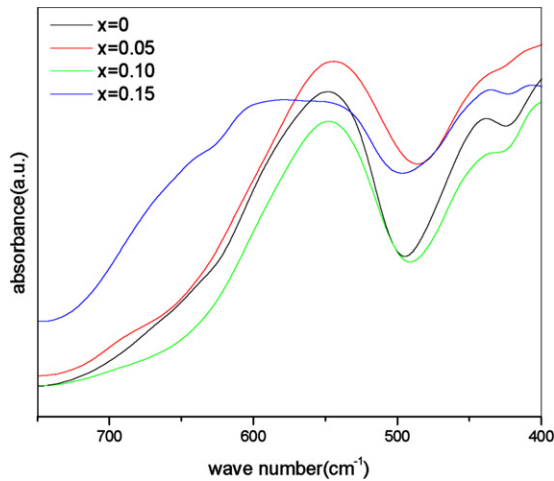


Figure 2. IR absorption spectra of $\text{Bi}_{1-x}\text{Y}_x\text{FeO}_3$.

form broadened peaks as the Y concentration increases. The calculated values of lattice parameters indicate that there is a continual change of lattice constant as a result of replacing the Bi^{3+} ion with the Y^{3+} ion. The change in value of c/a with Y substitution shows a change in crystal anisotropy with Y substitution in BFO. Also the increase in lattice strain with Y substitution introduces distortion in the rhombohedral structure in BFO. All these results together suggest that a structural transformation with a continual change of crystal structure parameters clearly occurs in BFO when Y substitution at the Bi site is increased.

The room temperature FTIR spectra are shown in figure 2. The strong absorption peaks near 547 cm^{-1} and another near 435 cm^{-1} are assigned to Fe–O stretching and bending vibration, respectively, being characteristics of the octahedral FeO_6 group in the perovskite compounds [27, 28]. As concluded earlier from XRD analysis, here also we see a clear departure of the FTIR spectra for $x = 0.15$ from the rest of the samples in terms of a very broad absorption peak near 547 cm^{-1} , which may be due to structural change in this material.

The frequency response of dielectric properties (figure 3) at 35°C shows a marked dispersive characteristic in both the permittivity and loss tangent pattern (figure 3 inset) of BFO, arising out of oxygen ion vacancies and consequent dc conductivity [29]. However, this behavior gets controlled in both permittivity and loss pattern for $x = 0.05\text{--}0.10$. This may be related to reduction of oxygen ion vacancies due to Y substitution (up to $x = 0.10$) in BFO. For $x = 0.15$ more dispersion in both permittivity and loss pattern along with their high values are observed. This may be due to the appreciable density of mobile charges in the sample and space charge polarization [30].

Figure 4 shows the temperature dependence of the dielectric permittivity (ϵ_r) and loss tangent ($\tan\delta$) (inset) of BYFO at 100 kHz. It clearly reflects an active role of Y concentration in modifying dielectric behavior of BFO. The permittivity versus temperature plot of BFO exhibits a small anomaly at 192°C , unlike in its $\tan\delta$ versus temperature plot

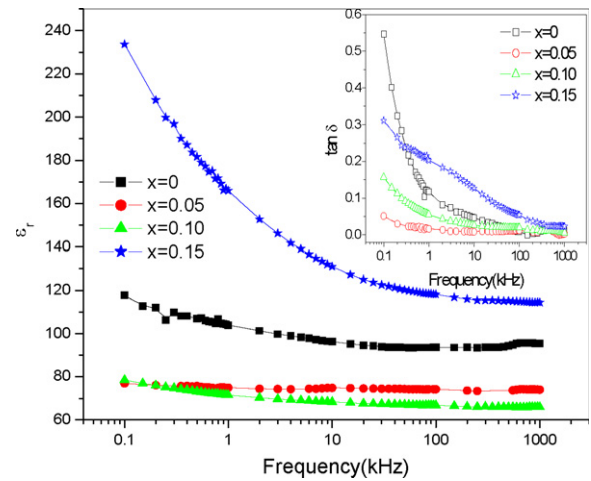


Figure 3. Variation of relative dielectric permittivity (ϵ_r) and loss tangent ($\tan\delta$) (inset) of $\text{Bi}_{1-x}\text{Y}_x\text{FeO}_3$ with frequency at 35°C .

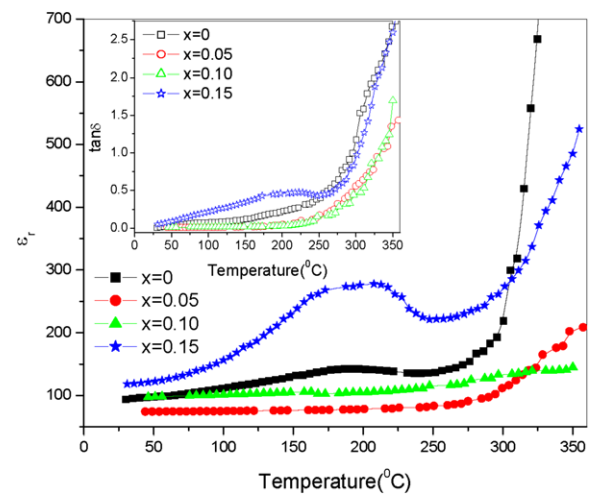


Figure 4. Variation of relative dielectric permittivity (ϵ_r) and loss tangent ($\tan\delta$) (inset) of $\text{Bi}_{1-x}\text{Y}_x\text{FeO}_3$ with temperature at a frequency of 100 kHz.

(i.e. a monotonic increase), which is consistent with the earlier report by Polomska *et al* [31]. It seems logical to attribute this anomaly to a transient interaction between oxygen ion vacancies and the $\text{Fe}^{3+}/\text{Fe}^{2+}$ redox couple. Replacement of Bi by Y ($x = 0.05\text{--}0.10$) modifies the dielectric characteristics of BFO, resulting in vanishing of the anomaly (at 192°C) and substantial reduction of $\tan\delta$. The replacement of some volatile Bi^{3+} with non-volatile Y^{3+} may prevent oxygen ion vacancies causing stabilization of the $\text{Fe}^{3+}/\text{Fe}^{2+}$ couple–oxygen vacancy interaction [11, 14]. However, further experiments like XPS are required for identification of the $\text{Fe}^{3+}/\text{Fe}^{2+}$ ratio. A contrasting and clearly marked feature was observed in the dielectric response for BYFO (i.e. $x = 0.15$) as indicated by diffused peaks in both the permittivity and loss tangent versus temperature pattern at 207°C and 222°C , respectively. Also for $x = 0.15$, in the entire range of temperature both permittivity and loss tangent are much higher than that of other compositions. The peaks in both permittivity (i.e. 207°C) and loss pattern for higher concentrations of Y

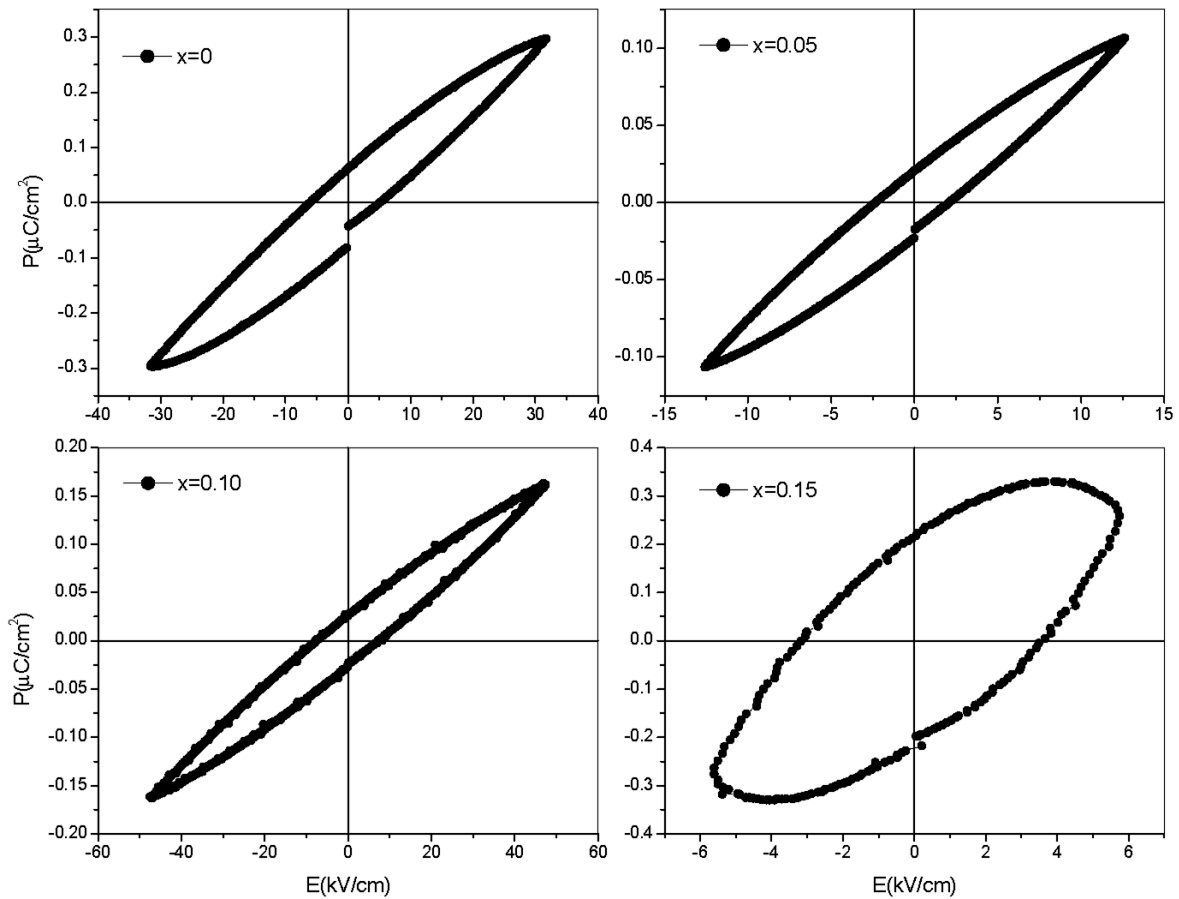


Figure 5. Room temperature P - E loop of $\text{Bi}_{1-x}\text{Y}_x\text{FeO}_3$.

($x = 0.15$) may be attributed to ferroelectric to paraelectric transition and/or magnetoelectric coupling. However, further analysis like DTA is required to establish this observation.

Figure 5 shows the variation of electric polarization (P) with applied electric field (E) of the poled samples of BYFO at room temperature. The P - E loops for all the samples were measured at a frequency of 20 Hz. Low values of remnant polarization are obtained in all the BYFO samples. Recently Singh *et al* [32] obtained saturated polarization in BFO thin film when measured at very high frequency. Here 15% Y substituted BFO clearly shows a very lossy behavior which is different from the rest of the sample.

The magnetization (M) versus temperature (T) of BYFO at 0.05 T under zero-field cooled (ZFC) and field-cooled (FC) conditions are shown in figure 6. Though the magnetization is small in BFO compared to the doped samples, there is a steep rise at lower temperatures. Such a rise in magnetization of BFO may arise from the impurity phase, the presence of Fe^{2+} ions and/or from the uncompensated spins at the surface of the antiferromagnetic systems which are natural for large surface to volume ratios when particle size becomes small [33]. The long-range cycloid order can also give rise to weak ferromagnetism [11, 21] and any disturbance to this spin arrangement may give rise to an increase in magnetization and a nonlinear field dependence at low T (as can be seen in the M - H curve at 2 K in figure 7). The magnetization was

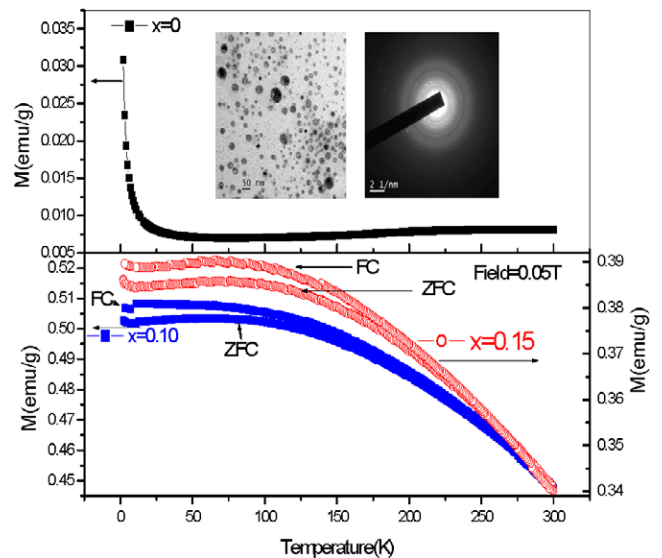


Figure 6. Magnetization (M) versus temperature (T) curve for $\text{Bi}_{1-x}\text{Y}_x\text{FeO}_3$ and a representative TEM-SAED pattern of BFO shown in the inset.

enhanced by an order of magnitude due to magnetic ordering on Y substitution for $x = 0.1$ - 0.15 . As such the magnetism of BFO is a long-standing problem and various controversial issues are arising from recent research on this system [34, 35].

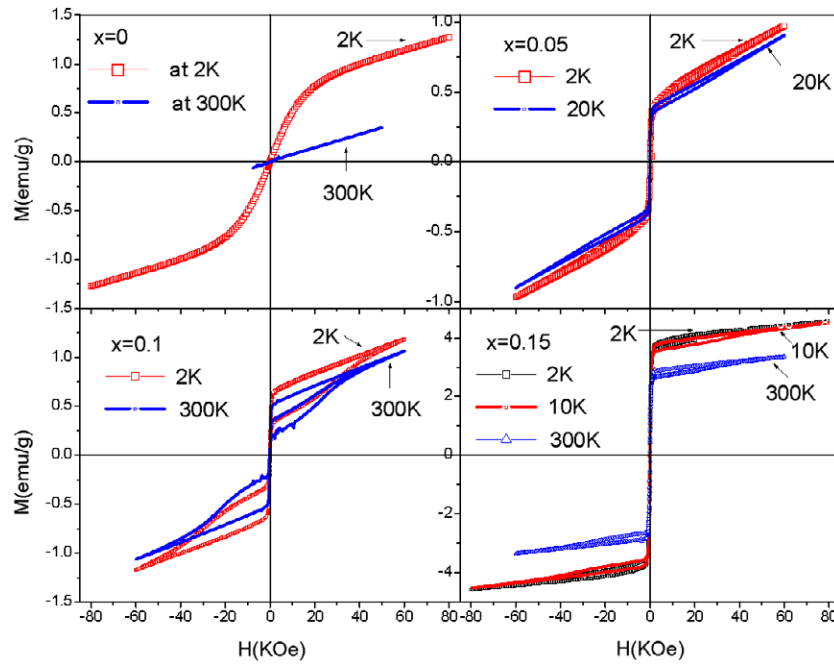


Figure 7. Magnetization (M) versus field (H) curve for $\text{Bi}_{1-x}\text{Y}_x\text{FeO}_3$ at different temperatures.

Doping of Y in BFO results in a very complicated scenario. We can envisage the following reasons for the enhancement in the bulk magnetization resulting from Y substitution: (i) change in the structure, (ii) variation in the oxygen stoichiometry or Fe^{2+} ion, (iii) reduction in particle size to the range of the modulation length of the spin cycloid (~ 62 nm), (iv) change in the magnetic anisotropy etc. It was shown recently that nanoparticles of BFO show high saturation magnetization and a ferromagnetic hysteresis loop even in room temperature [36]. It is well known that BFO has G-type antiferromagnetic order with a long period of ~ 62 nm of canted spins between the two successive ferromagnetically coupled (111) planes [21]. This periodicity of the spin cycloid can be broken in small particles when their size is reduced to around or below 62 nm, which will enhance magnetization. In the present study, the average particle size in the whole series is less than the long-range cycloid order. Such incomplete order will result in inhomogeneity in the system which is evident from the bifurcation of ZFC and FC magnetization in $Y = 0.1$ and 0.15 samples (figure 6) which have particle sizes smaller than BFO.

The combined effect of all the above mentioned factors results in very interesting behavior of the magnetization as a function of field, as shown in figure 7. A systematic change in the $M-H$ loops results in the BYFO samples from a straight line to a sizable loop on increasing Y content. Though the room temperature $M-H$ loop is linear for BFO, there is a considerable deviation from linearity at 2 K. The effect of a small amount of Y is clearly perceptible in the evolution of the hysteresis loop, imparting a switchable behavior of BYFO in the temperature range of 2–300 K. All the Y doped samples show a sudden increase in M in low fields followed by an almost linear increase, reminiscent of the field dependence of antiferromagnetic systems. The sample with $Y = 0.1$ also shows a metamagnetic transition around a field which increases

with decrease in temperature. This is a typical signature of field induced alignment of spins in an AFM system opening the hysteresis loop. Though the samples with $Y = 0.05$ and 0.15 also have signatures of similar metamagnetic behavior and opening in the hysteresis loop, they appear weak on the same scale. However, the switching behavior in low fields is the most interesting observation of the field dependence of magnetization which occurs even at room temperature. This unique observation is rather intriguing for this multiferroic system and needs to be addressed by further studies using both macroscopic and microscopic tools.

4. Conclusion

It is concluded that Y substitution at the Bi site of BFO has caused compositionally driven structural change and facilitates single phase formation of the material by suppressing the pyrochlore phase. This has led to a considerable change in dielectric, ferroelectric and magnetic properties of BFO. Up to 10% Y substitution there is a significant reduction of low frequency dispersion in both permittivity and loss pattern, indicating a considerable control of dc conductivity thereby enhancing ferroelectric behavior. Also up to 10% Y substitution the permittivity and loss value remain stable in a wide range of temperature, which is not observed in the case of rare earth substituted BFO. Unlike rare earth substituted BFO, one of the distinguishing feature observed in the present study is the anomaly in the variation of dielectric permittivity and loss tangent with temperature for 15% Y substituted BFO at around 207°C . This anomaly may be attributed to ferro- to paraelectric transition and/or magnetoelectric coupling. It has been established before that any substitution at the Bi site in BFO results in suppression of the spin cycloid and enhances

macroscopic magnetization. However, with Y substitution at the Bi site we get remarkable increase in macroscopic magnetization and the switching behavior in low fields which is the most interesting observation of the field dependence of magnetization of BYFO samples, which makes them different from rare earth substituted BFO. More importantly this occurs even at room temperature. This unique magnetic behavior along with the existence of ferroelectricity in these samples makes them probable candidates for obtaining better magnetoelectric coupling.

Acknowledgments

The authors acknowledge DST, Govt of India for funding the VSM. One of the authors (R K Mishra) expresses gratitude to Govt of Orissa and the principal of his parent college, V N College, Jajpur Road, Orissa for grant of study leave and Dr Shrabanee Sen (NML, India) for some help in experimental work.

References

- [1] Hill N A 2000 *J. Phys. Chem. B* **104** 6694
- [2] Eerenstein W, Mathur N D and Scott J F 2006 *Nature* **442** 759
- [3] Prellier W, Singh M P and Murugavel P 2005 *J. Phys.: Condens. Matter* **17** R803–32
- [4] Kumar M M, Palkar V R, Srinivas K and Suryanarayan S V 2004 *Appl. Phys. Lett.* **84** 1731
- [5] Palkar V R, John J and Pinto R 2002 *Appl. Phys. Lett.* **80** 1628
- [6] Cheng J R, Li N and Cross L E 2003 *J. Appl. Phys.* **94** 5153
- [7] Venevtsev Yu N and Gagulin V V 1994 *Ferroelectrics* **162** 23
- [8] Chen F, Zhang Q F, Li J H, Qi Y J, Lu C J, Chen X B, Ren X M and Zhao Y 2006 *Appl. Phys. Lett.* **89** 092910
- [9] Shvartsman V V, Kleemann W, Haumont R and Kreisel J 2007 *Appl. Phys. Lett.* **90** 172115
- [10] Palkar V R, Kundaliya Darshan C and Malik S K 2003 *J. Appl. Phys.* **93** 4337
- [11] Huang F, Lu X, Lin W, Wu X, Kan Yi and Zhu J 2006 *Appl. Phys. Lett.* **89** 242914
- [12] Kim J S, Cheon C II, Lee C H and Jang P W 2004 *J. Appl. Phys.* **96** 468
- [13] Murashov V A, Rakov D N, Ionov V M, Dubenko I S and Titov Y V 1994 *Ferroelectrics* **162** 11
- [14] Hiroshi U, Risako U, Hiroshi F and Koda S 2006 *J. Appl. Phys.* **100** 014106
- [15] Das S R, Bhattacharya P, Choudhary R N P and Katiyar R S 2006 *J. Appl. Phys.* **99** 066107
- [16] Yuan G L, Or S W and Chan H L Wa 2007 *J. Phys. D: Appl. Phys.* **40** 1196
- [17] Gabbasova Z V, Kuz'min M D, Zvezdin A K, Dubenko I S, Murashov V A, Rakov D N and Krynetsky I B 1991 *Phys. Lett. A* **158** 491
- [18] Ederer C and Spaldin Nicola A 2005 *Phys. Rev. B* **71** 224103
- [19] Zalesskii A V, Frolov A A, Khimich T A and Bush A A 2003 *Phys. Solid State* **45** 141
- [20] Zhang S-T, Pang L-H, Zhang Y, Lu M-H and Chen Y-F 2006 *J. Appl. Phys.* **100** 114108
- [21] Kadomtseva A M, Popov Yu F, Pyatakov A P, Vorob'ev G P, Zvezdin A K and Viiehlend D 2006 *Phase Transit.* **79** 1019
- [22] Bhat M, Kaur B, Kumar R, Joy P A, Kulkarni S D, Bamzai K K, Kotru P N and Wanklyn B M 2006 *Nucl. Instrum. Methods Phys. Res. B* **243** 134
- [23] Treves D 1965 *J. Appl. Phys.* **36** 3
- [24] POWDMULT: An interactive powder diffraction data interpretations and indexing Program Version 2.1 *E. WU School of Physical Sciences Flinder University of South Australia Bradford Park SA 5042, Australia*
- [25] Wilson A J C 1962 *Proc. Phys. Soc.* **80** 286
- [26] Klug P Harold and Alexander Leroy E 1973 *X-ray Diffraction Procedures for Polycrystalline and Amorphous Materials* (New York: Wiley)
- [27] Subba Rao G V and Rao C N R 1970 *Appl. Spectrosc.* **24** 436
- [28] Chen C, Cheng J, Yu S, Che L and Meng Z 2006 *J. Cryst. Growth* **291** 135
- [29] Jonscher A K 1977 *Nature* **267** 673
- [30] Jonscher A K, Meca F and Millany H M 1979 *J. Phys. C: Solid State Phys.* **12** L293
- [31] Polomska M, Kaczmerk W and Pajak Z 1974 *Phys. Status Solidi a* **23** 567
- [32] Singh S K, Maruyama K and Ishiwara H 2007 *J. Phys. D: Appl. Phys.* **40** 2705
- [33] Nair Sunil and Banerjee A 2004 *Phys. Rev. Lett.* **93** 117204
- [34] Wang J, Neaton J B, Zheng H, Nagarajan V, Ogale S B, Liu B, Viehland D, Vaithyanathan V, Scholm D G, Waghmare U V, Spaldin N A, Rabe K M, Wuttig M and Ramesh R 2003 *Science* **299** 1719
- [35] Eerenstein W, Morrison F D, Dho J, Blamire M G, Scott J F and Mathur N D 2005 *Science* **307** 1203
- [36] Mazumder R, Sujatha Devi P, Bhattacharya D, Choudhury P, Sen A and Raja M 2007 *Appl. Phys. Lett.* **91** 062510